

## Relativistic Energy-Band Structure of $Mg_2Pb$

J. P. Van Dyke\*

Sandia Laboratories, Albuquerque, New Mexico 87115

and

Frank Herman

IBM Research Laboratory, San Jose, California 95114

(Received 18 May 1970)

The energy-band structure of  $Mg_2Pb$  as calculated by the relativistic orthogonalized-plane-wave method is described. The valence-band edge is found to be at the zone center and the conduction-band edge at the zone boundary, probably at the point  $X$ . Band parameters are calculated and compared with recent Fermi-surface data.

In this paper we present the results of a first-principles calculation of the relativistic energy-band structure of magnesium plumbide. To our knowledge, this is the first energy-band calculation for  $Mg_2Pb$ , although the first three materials of the series  $Mg_2X$ , where  $X$  is Si, Ge, Sn, and Pb, have been previously investigated.<sup>1-4</sup> These four compounds which crystalize in the antifluorite structure have band gaps that decrease from Si through Pb.  $Mg_2Pb$  is a semimetal.<sup>5,6</sup> However, semiconducting properties have been reported for crystals from the Mg-Pb system.<sup>7</sup> The presence of a second nearly stoichiometric phase in the recently determined Mg-Pb phase diagram<sup>8</sup> explains the discrepancy.<sup>6</sup>

The crystal potential model for this fully relativistic orthogonalized-plane-wave (ROPW) calculation<sup>9-11</sup> is the exact analog of the nonrelativistic model described by Herman and Skillman.<sup>12</sup> The crystal potential is made up of superimposed self-consistent relativistic free-atom potentials.<sup>13</sup> The Kohn-Sham-Gaspar version of the Hartree-Fock-Slater free-electron exchange approximation is employed. This model successfully describes the energy-band structure of relativistic IV-VI semiconductor compounds<sup>11</sup> and of the semimetal grey tin.<sup>14</sup>

The energy-band structure of  $Mg_2Pb$  is shown in Fig. 1. The over-all energy-band structure of the  $Mg_2X$  compounds is remarkably like column IV or III-V semiconductors. In addition to the band overlap  $Mg_2Pb$  differs from the other  $Mg_2X$  materials in having larger spin splittings and larger relativistic shifts of  $s$ -like levels.<sup>15</sup> The calculated ROPW values are shown as circled dots, and the curves are drawn free hand, guided by connectivity rules and the known energy bands<sup>4</sup> of the other compounds in the  $Mg_2X$  series. Energies near the Fermi energy at the symmetry points are listed in Table I.

In  $Mg_2Pb$  there is experimental evidence<sup>16</sup> for

both holes and electrons. The calculated energy-band structure unambiguously shows the valence-band edge to be  $\Gamma_8^-$ . (This would be so even if  $\Gamma_8^+$  were below  $\Gamma_8^-$  as in grey tin.<sup>14</sup>) Thus, we can definitely place the holes at  $\Gamma$ . The electrons can be concentrated either at  $X$  or  $L$  but are unlikely to be found elsewhere. We find conduction-band minima at  $\Gamma$ ,  $X$ , and  $L$ . The calculated gaps from  $\Gamma_8^-$  are 0.15 eV at  $\Gamma$  and  $L$ , but there is a 0.01-eV overlap at  $X$ . Although our calculation indicates that  $Mg_2Pb$  is semimetallic in agreement with experiment,<sup>5,6,16</sup> the calculational uncertainties exceed the band overlap. Extrapolating from  $Mg_2Si$  and  $Mg_2Ge$ , Lee<sup>2</sup> predicted that the holes

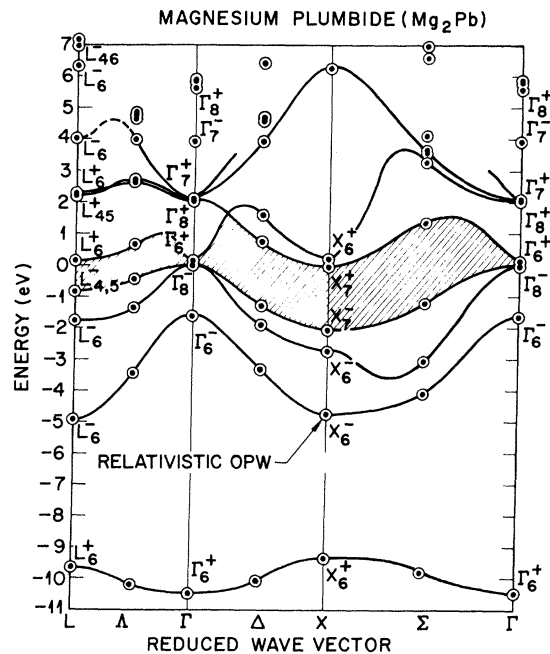


FIG. 1. Energy-band structure of  $Mg_2Pb$ . The curves are drawn free hand.

TABLE I. Calculated energy levels in Mg<sub>2</sub>Pb in eV.<sup>a</sup>

$\Gamma_{25'}$	$\Gamma_7^+$	2.10	$X_1$	$X_6^+$	0.22	$L_3$	$L_6^+$	2.30
	$\Gamma_8^+$	2.07					$L_{45}^+$	2.25
$\Gamma_1$	$\Gamma_6^+$	0.15	$X_3$	$X_7^+$	-0.014		$L_6^+$	0.16
$\Gamma_{15}$	$\Gamma_8^-$	0.00	$X_5$	$X_7^-$	-2.09	$L_{3'}$	$L_{45}^-$	-0.86
	$\Gamma_6^-$	-1.66					$L_6^-$	-1.74

<sup>a</sup>The lattice constant used was 12.9183 a.u.

would be at  $\Gamma$  and the electrons at  $X$ .

Since the valence-band edge  $\Gamma_8^-$  is a twofold level (fourfold with spin), there are two bands associated with it. We have calculated band curvatures for both bands at  $\Gamma$  and for the conduction-band edges at  $X$ . We have also investigated the anisotropy of the bands at  $\Gamma$ .

The calculated heavy hole band is described quite well up to the estimated Fermi energy by the dispersion relation  $E = k^2 f(\theta, \varphi)$ , where  $f(\theta, \varphi)$  is independent of the magnitude of  $k$  and, hence, the band curvature is independent of  $E$ . The calculated band masses are listed in Table II. For comparison with cyclotron masses, the band masses were averaged about an assumed central orbit using for the angular dependence (of the inverse mass) the simplest trigonometric form consistent with the orbit. [If the above dispersion relation is valid,  $f(\theta, \varphi)$  describes the angular variation of the inverse mass.] The calculated average masses are listed in Table II, as are Stringer and Higgins's experimental values for the cyclotron mass. From their measured areas, Stringer and Higgins deduce values for the Fermi radius. We have carried out a full ROPW calculation at their values for  $k_F$  along principal directions. These energies and their values of  $k_F$  are listed in Table II. We also list the anisotropy of their  $k_F$  values along with the anisotropy which we deduce using the above dispersion relation and the calculated energies.

The calculated mass of the light hole band is about  $0.015m_0$  at the top of the band and about  $0.03m_0$  at the Fermi energy. The light hole band

TABLE III. Calculated conduction-band effective masses at  $X$  in Mg<sub>2</sub>Pb.<sup>a</sup>

	$X_7^+$	$X_6^+$
$m_{L}^*/m_0$ <sup>b</sup>	1.10	0.58
$m_{T}^*/m_0$ <sup>c</sup>	0.25	0.16

<sup>a</sup>In units of free-electron mass calculated from energy about 1% of the Brillouin-zone radius away from  $X$ .

<sup>b</sup>Longitudinal mass.

<sup>c</sup>Transverse mass.

is strongly coupled to the  $\Gamma_6^+$  band, and, thus, any uncertainty in the  $\Gamma_6^+ - \Gamma_8^-$  gap would be reflected in the value found for the light hole mass. (The heavy holes are much less sensitive to the gap.<sup>17</sup>) The light holes are nearly isotropic but highly non-parabolic. In fact, the calculated light hole band and the  $\Gamma_6^+$  band are described quite well by a two-band isotropic model. The two-band analysis implies that to agree with the light hole area of Stringer and Higgins (and the Fermi energy we find for heavy holes) the  $\Gamma_6^+ - \Gamma_8^-$  gap should be  $0.30 \pm 0.10$  eV, compared to the calculated value  $0.14$  eV. This value of the gap is also consistent with the experimental mass value. This does determine the  $\Gamma_6^+$  level to be above  $\Gamma_8^-$ .

The location of the electron Fermi-surface piece has not been determined experimentally. Theoretically, we cannot rule out the  $L_6^+$  level; however, the  $X_7^+$  state is the more likely candidate. The masses for the conduction bands at  $X$  are listed in Table III. If the electrons are associated with the  $X_7^+$  states, we would expect, on the basis of the mass estimates and compensation (which Stringer and Higgins do observe), that the  $\Gamma_8^- - X_7^+$  overlap should be  $0.15 \pm 0.05$  eV, compared to the calculated  $0.01$  eV.

Assuming the  $X_7^+$  state to be the conduction-band edge, the first-principles energy-band structure leads to key gaps which are correct to within  $0.2$  eV.

We are preparing to calculate optical properties

TABLE II. Parameters of the heavy holes in Mg<sub>2</sub>Pb.

	Theory <sup>a</sup>	Expt. <sup>b</sup>	Theory <sup>c</sup>	SH <sup>d</sup>		SH <sup>b</sup>	Theory
	$m^*/m_0$	$m_c^*/m_0$	$m_{av}^*/m_0$	$k_F$	$E(k_F)$ <sup>e</sup>	$k_F/k_{110}$	$k_F/k_{110}$
100	0.25	$0.35 \pm 0.02$	0.35	0.0692	0.07218	0.633	0.722
110	0.49	$0.45 \pm 0.06$	0.46	0.1093	0.09376	1.0	1.0
111	0.65	$0.45 \pm 0.06$	0.43	0.1262	0.08757	1.155	1.196

<sup>a</sup> $(m^*/m_0)^{-1}$  is the curvature in the given direction calculated from the energy about 1% of the Brillouin-zone radius away from  $\Gamma$ .  $m_0$  is the free-electron mass.

<sup>b</sup>Reference 16.

<sup>c</sup> $m^*/m_0$  averaged over a central orbit perpendicular to the given direction. (See text for averaging details.)

<sup>d</sup>From Ref. 16 in wave number units,  $\text{\AA}^{-1}$ .

<sup>e</sup>Calculated energy at the listed value of  $k_F$ .

( $\epsilon_2$ ) for  $\text{Mg}_2\text{Pb}$ . It is to be hoped that the publishing of this band structure plus the resolution of the crystal preparation problem<sup>6</sup> will stimulate the measurement of optical properties of  $\text{Mg}_2\text{Pb}$  like the reflectivity<sup>18</sup> and modulated reflection<sup>19</sup> work

that has been done on the other  $\text{Mg}_2X$  compounds.

The authors are grateful to Dr. G. A. Stringer and Professor R. J. Higgins for communicating their experimental results in advance of publication.

\*Work supported by the U. S. Atomic Energy Commission.

<sup>1</sup>N. O. Folland, Phys. Rev. **158**, 764 (1967).

<sup>2</sup>P. M. Lee, Phys. Rev. **135**, A1110 (1964).

<sup>3</sup>M. Y. Au-Yang and M. L. Cohen, Phys. Rev. **178**, 1358 (1969).

<sup>4</sup>J. P. Van Dyke, F. Herman, and R. L. Kortum (unpublished).

<sup>5</sup>U. Winkler, Helv. Phys. Acta **28**, 633 (1955).

<sup>6</sup>G. A. Stringer and R. J. Higgins, J. Appl. Phys. **41**, 489 (1970).

<sup>7</sup>G. Busch and M. Moldovanova, Helv. Phys. Acta **35**, 500 (1962).

<sup>8</sup>J. M. Eldridge, E. Miller, and K. L. Komark, Trans. AIME **233**, 1303 (1965).

<sup>9</sup>P. Soven, Phys. Rev. **137**, A1706 (1965).

<sup>10</sup>I. B. Ortenburger and F. Herman, Bull. Am. Phys. Soc. **13**, 413 (1968).

<sup>11</sup>F. Herman, R. L. Kortum, I. B. Ortenburger, and J. P. Van Dyke, J. Phys. (France) **29**, C4-62 (1968).

<sup>12</sup>F. Herman and S. Skillman, in *Proceedings of the International Conference on Semiconductor Physics*,

Prague, 1960 (Academic, New York, 1961), p. 20.

<sup>13</sup>D. Liberman, J. T. Waber, and D. T. Cromer, Phys. Rev. **137**, A27 (1965).

<sup>14</sup>F. H. Pollack, M. Cardona, C. W. Higginbotham, F. Herman, and J. P. Van Dyke, Phys. Rev. B **2**, 352 (1970).

<sup>15</sup>The relativistic shift of conduction-band-edge  $s$  levels is  $\Gamma_6^+(\Gamma_1)$ , 2.0 eV;  $X_3^+(X_3)$ , -0.50 eV;  $L_4^+(L_1)$ , 0.53 eV. These shifts are with respect to the center of gravity of  $\Gamma_6^-$  and  $\Gamma_8^-(\Gamma_{15})$  and are differences from the same crystal model nonrelativistically. The negative shift of the Mg  $s$ -like  $X_3$  level was also found in  $\text{Mg}_2\text{Sn}$  (-0.15 eV). The  $X_1$  state did not shift relativistically in  $\text{Mg}_2\text{Pb}$  or  $\text{Mg}_2\text{Sn}$ .

<sup>16</sup>G. A. Stringer and R. J. Higgins, Phys. Rev. (to be published).

<sup>17</sup>If the coupling between  $\Gamma_6^+$  and  $\Gamma_8^-$  is examined in first order  $\mathbf{k} \cdot \mathbf{p}$ ,  $\Gamma_6^+$  and the light holes are isotropically coupled, but the heavy holes are not coupled to  $\Gamma_6^+$  at all.

<sup>18</sup>W. J. Scouler, Phys. Rev. **178**, 1359 (1969).

<sup>19</sup>F. Vazquez, R. A. Formun, and M. Cardona, Phys. Rev. **176**, 905 (1969).

## Simultaneous Generation of Transition Radiation and Bremsstrahlung from a Thin Foil. I\*

S. Y. Shieh<sup>†</sup>

*Department of Physics and Astronomy, University of Tennessee, Knoxville, Tennessee 37916*

and

R. H. Ritchie

*Health Physics Division, Oak Ridge National Laboratory, Oak Ridge, Tennessee 37830*

and

*Department of Physics and Astronomy, University of Tennessee, Knoxville, Tennessee 37916*

(Received 10 February 1970)

The usual procedure of reducing transition-radiation data by simply subtracting bremsstrahlung yield from the total yield ignores the coherent interference effect between transition radiation and bremsstrahlung. Assuming single scattering, we have analyzed the simultaneous generation of transition radiation and bremsstrahlung of a charged particle normally incident on a thin slab. The results obtained here not only should be useful for reducing experimental data on transition radiation, but also should provide a new independent means to deduce the mean-square angle for single scattering.

### I. INTRODUCTION

When a charged particle passes through a thin dielectric slab without deflection along the direction of the normal to the plane surfaces of the slab, transition radiation with its characteristic polar-

ization will be emitted.<sup>1</sup> Transition radiation from a normally incident charged particle is always polarized in the plane of emission determined by the direction of observation and the normal to the slab. However, in practice charged particles may suffer scattering in the slab, in which case